AN AXISYMMETRIC NONLINEAR TRANSIENT THERMO-ELASTIC WINDING MODEL

By

C. Mollamahmutoglu[1] and J. K. Good[2]
[1]Yildiz Technical University, TURKEY
[2]Oklahoma State University, USA

ABSTRACT

Temperature is among the most important environmental factors which play a crucial role on the mechanical state of wound rolls of web material. Existing literature include studies concerning the thermal characterization of the web materials and the effects of spatially homogeneous temperature change for the entire roll in the realm of 1D plane stress/strain thermos-elastic winding models. These 1D models have been verified and have proven that internal roll stresses are very sensitive to the amplitude of the homogenous temperature change. Homogenous temperature changes are not a physical reality. The temperature distribution in a wound roll will vary dynamically through time as the wound roll moves from one thermal environment to another. To capture the dynamic variation in temperature the heat-diffusion differential equation is solved in axisymmetric form. Although it is expected that the thermal conductivity will be highly orthotropic in the wound roll and that there may be state dependency on contact pressure, as an initial approach to the problem, thermal conductivity is assumed to vary with respect to position only. After solving the heat-diffusion model in axisymmetric form, obtained temperature variation through time in the axisymmetric r-z plane can be used within a thermo-elastic axisymmetric winding model. Within the axisymmetric thermo-elastic winding model temperature variation will result in contact pressure variation. This will result in variation of the radial modulus of elasticity which is known to be state dependent on contact pressure. Thus, taking into account this nonlinearity, an incremental thermo-elastic analysis is applied for a given transient heat response. The heat-diffusion and thermo-elastic models will be used consecutively and the stress states are calculated as the wound roll moves from thermal equilibrium in one environment to another. Explorations of how axisymmetric roll stresses vary while the wound roll achieves thermal equilibrium will be presented.

INTRODUCTION

Temperature change causes thermal expansion or shrinkage hence fundamentally affects the stress state of a wound roll [1]. Although an important number of related engineering problems can be solved assuming steady-state conditions, in reality temperature changes are dynamical. This is especially important in winding problems where radial modulus is pressure dependent and pressures are in turn affected by spatially inhomogeneous temperature distribution. Thus a thorough analysis of temperature distribution over time is required for correct assessment of the mechanical state of a wound roll. Literature include studies concerning the thermal characterization of web materials and 1D models which assume thermo-elastic solutions based on homogeneous temperature distribution. These, experimentally verified, 1D thermo-elastic models revealed the sensitivity of the stress state to the amplitude of homogeneous temperature change. In order to take into account material nonlinearity, these simple models are based on numerical solution techniques such as finite differences and can only produce stress variations along radial and tangential directions [1]. In order to obtain axial and shear stresses a higher dimensional model geometry is required. Although true representation of the geometry of a wound roll would be a 3D spiral structure, current computational power of numerical solution systems arguably dictates an axisymmetric cylindrical structure as the most convenient way of representing a roll. Axisymmetric models can be thought as 2D models where layers are taken as concentric hoops shrink fit over a cylinder core. Early 2D models were simple extension of 1D models as they were formed by stacking multiple 1D models along axial direction [3]. Later real 2D models appeared which directly formulated the axisymmetric domain thus naturally incorporating the physical continuity along axial direction [4]. These models can produce full axisymmetric stress field including the axial and shear components even for very soft materials which require nonlinear geometrical formulation [5]. Therefore, in a true axisymmetric model, without complicating the geometry in tangential direction, most of the crucial features regarding to mechanical state such as effects of wide-wise or length-wise thickness variation, shear slippage and buckling along axial direction can be captured and studied. The axisymmetric winding model proposed by authors, [2] is state-of-the-art and besides features mentioned above it can also effectively deal with the so called tension loss effect [6]. With these advancements there is still an existing gap in the literature where thermo-elastic problems for wound rolls arise. Axisymmetric winding problem which is concerning the thermal effects whether steady or transient has not been encountered in existing literature. During storage or production stages wound rolls are often experiences different temperatures and a thorough analysis is required. In this study this task is undertaken by proposing an axisymmetric transient heat-diffusion model which is integrated to the winding model developed by the authors [2]. The main assumption is all thermal processes will start after the winding ends. The development plan will be as following: In the first section we will briefly describe essentials of the axisymmetric winding formulation. The second section will be concerned with the development of the thermo-elastic stress analysis of a wound roll. This section will serve as the connection between the heat transfer and the stress problems by relating the incremental stress response to the incremental temperature changes. In the third section transient heat transfer essentials for the axisymmetric domain will be reviewed. Temperature distribution results of heating/cooling of wound rolls will be demonstrated and compared with the results obtained by a commercial finite element package. Forth section is devoted to the numerical results obtained from a code which is developed on the ideas of the previous sections. For this purpose an efficient general integrated algorithm for the

heat-transfer and stress calculations is given. In this section comparisons of the developed model with existing 1D thermo-elastic experimental results are shown. Effect of wide-wise thickness variation, assuming orthotropic, inhomogeneous thermal conductivity are also studied. Final section includes discussion and recommendations on possible future research directions.

AXISYMMETRIC WINDING MODEL

Per our main assumption, all thermal effects will start right after the winding ends. That is winding is done under isothermal conditions and effects take place when roll is immersed into a different temperature medium. Thus we need a precise knowledge of the mechanical state of the newly wounded roll as it will set the initial conditions for thermo-elastic analysis. In our previous study we have proposed a novel 2D axisymmetric wound roll formulation [2]. The details can be found in the mentioned study but we will repeat some essential information here for the sake of completeness. In 2D axisymmetric formulation the finite width wound roll is represented via concentric hoops of web each representing a layer. A layer in turn is modeled as a series of 4-node quadrilateral elements along CMD. The thickness variation is imposed at the layer level by changing the quad elements dimensions according to the thickness data. This allows approximating the thickness by means of piece-wise linear functions along CMD. In Figure 1 a general depiction of the model is shown.

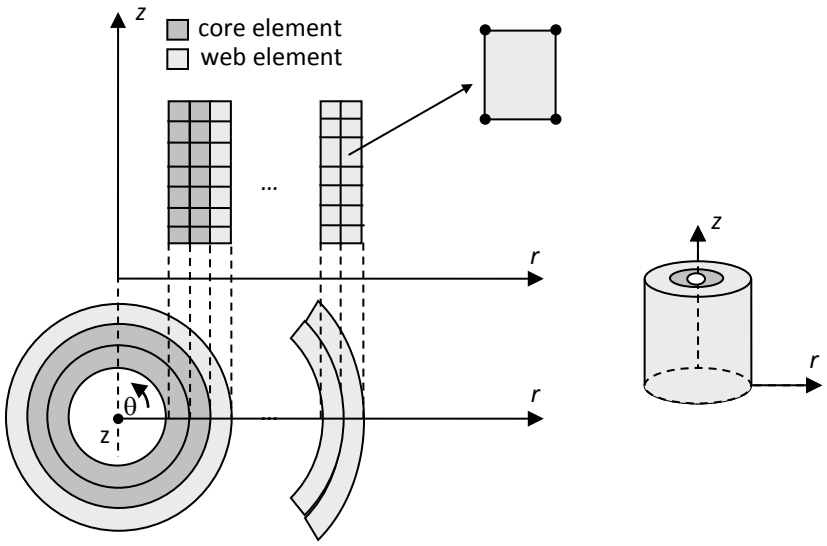

Figure 1 – Modeling of Wound Rolls with Axisymmetric Finite Elements

Typical isoparametric displacement based finite element formulation is used with the 4-node quad elements. The master and actual elements are shown in Figure 2. As observed on actual element side lengths h_1 and h_2 are controlling the thickness variation across the element whereas node positions r_1 and r_2 controls the radial position.

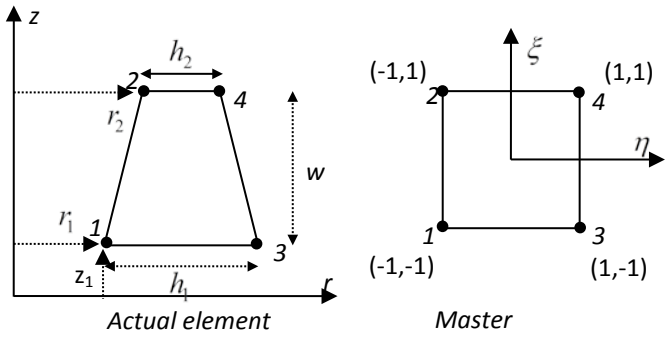

Figure 2 – Actual *r-z* and Natural η-ξ Coordinates for an Axisymmetric Finite Element

Figure 3 shows a typical instance in the *r-z* plane during winding with CMD thickness variation. The resulting non-uniform roll profile will dictate the shape of the outer layer as it is winding over the roll. In Figure 3 it is also possible to see a generic sector (j^{th} element) with thickness variation over it.

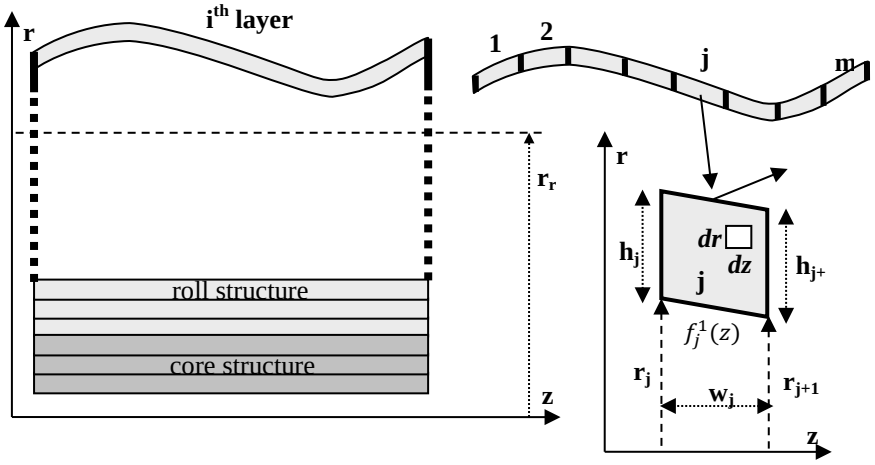

Figure 3 – Treatment of the Outer Lap Using a Pre-Stress Formulation: Thickness Variation

The details of the general derivation of the finite element equations {1} omitted here. After carrying out the usual procedures for the element stiffness matrix K_e and force vector F_e we obtain equations {2} and {3}:

$$K_e u_e = F_e \qquad \{1\}$$

$$K_e = \int_{-1}^{1}\int_{-1}^{1} B^T M_e B \det[J] r d\eta d\xi \qquad \{2\}$$

$$F_e = -\int_{-1}^{1}\int_{-1}^{1} B^T \sigma_0 \det[J] r d\eta d\xi \qquad \{3\}$$

In {1} u_e is the 8x1 element displacement vector. In {2} and {3} *B* is the usual small strain-displacement matrix, det[*J*] is the determinant of the Jakobien *J*, *r* is the radial position. M_e is the material stiffness matrix with subscript e is for "element" and superscript *t* denotes transpose. The material stiffness matrix M_e is simply the inverse of the compliance matrix C_e:

$$C_e = \begin{bmatrix} 1/E_r & -\upsilon_{rz}/E_z & 0 & -\upsilon_{r\theta}/E_\theta \\ -\upsilon_{rz}/E_z & 1/E_z & 0 & -\upsilon_{z\theta}/E_\theta \\ 0 & 0 & 1/G_{rz} & 0 \\ -\upsilon_{r\theta}/E_\theta & -\upsilon_{z\theta}/E_\theta & 0 & 1/E_\theta \end{bmatrix} = \mathrm{INV}[M_e] \qquad \{4\}$$

Here Maxwell's relations are imposed ($\upsilon_{zr}/E_r = \upsilon_{rz}/E_z$, $\upsilon_{\theta r}/E_r = \upsilon_{r\theta}/E_\theta$, $\upsilon_{\theta z}/E_z = \upsilon_{z\theta}/E_\theta$). One important aspect here is the radial modulus E_r which is state dependent i.e. $E_r=E_r(\sigma_r)$. One of the most common forms used for E_r in web handling research is due to Pfeiffer:

$$E_r = K_2(-\sigma_r + K_1) \qquad \{5\}$$

Here K_1 and K_2 are the well-known material specific Pfeiffer constants. The pressure increases monotonically due to addition of a layer so E_r of the element changes during winding. Winding is inherently layer-wise and we took advantage of this by employing a step wise linearization, i.e. addition of a layer is taken as a step. During solution of a step radial moduli of elements are kept constant and they are only updated after the incremental stress change is calculated and the total stresses are updated at the end of the solution for that step. Thus the equations are solved as many times as the number of layers within a roll. The incremental stresses resulting from addition of a layer is calculated and the total stress state is updated and finally radial moduli of elements are recalculated per {5} at the end of the step. As discussed in [2] this approach proved accurate results without resorting more complicate Newton-Raphson type linearization techniques.

The most important part of the winding formulation is the pre-stress formulation which has resulted in equation {3}. In {3} σ_0 is the initial stress due to web line tension. Selecting an appropriate σ_0 vector for an element in order to simulate the effect of thickness variation is based on the notion of relaxation radius [2]. Briefly, in {6} the mechanical equilibrium of the outer lap is written: Left hand side is the total web line force written over web line tension T_w. Here A_j is the area of the sector *j* (refer Figure 3). Right hand side is the total web line force written over the applied stretch due to roll profile. Here $E_{\theta j}$ is the tangential modulus for sector *j* and f_j functions are defined in Figure 3. The stretch is causing a strain (integrand) which in turn relates to corresponding stress for typical sector *j*. Key point is expressing the tangential strain via utilizing the relaxation radius r_r which denotes the tension free radius of a layer of web. This approach naturally allows incorporation of the effect of roll profile.

$$T_w \sum_{j=1}^{m} A_j = \sum_{j=1}^{m} E_{\theta j} \int_0^{w_j} \int_{f_j^1(z)}^{f_j^2(z)} \frac{r - r_r}{r_r} dr dz \quad \{6\}$$

Once relaxation radius r_r from {6} is solved it can be inserted into equation {7} and the appropriate pre-stress vector σ_0 for the simulation of the effect of CMD thickness non-uniformity can be obtained.

$$(\sigma_0)^j = \begin{bmatrix} 0 & 0 & 0 & -E_{\theta j} \frac{r_j - r_r}{r_r} \end{bmatrix}^t \quad \{7\}$$

At the end of winding session we obtain the total stress and strain state which will be used as initial conditions for the post-winding thermal stresses.

THERMO-ELASTIC ANALYSIS OF A WOUND ROLL

Temperature change simply results in thermal expansion which in turn causes thermal strains. In its simplest form relation between stress change and temperature change is linear. We will use an incremental form of this relation because of material nonlinearity. We may consider an incremental stress corresponding to an incremental change in temperature:

$$\Delta {\sigma_e}^k = M^{k-1}(\Delta {\varepsilon_e}^k - \Delta \varepsilon_{thermal}) \quad \{8\}$$

Here $\Delta {\sigma_e}^k$ and $\Delta {\varepsilon_e}^k$ are the element incremental stress vector and incremental total strain vector respectively for step a time step *k*. $\Delta \varepsilon_{thermal}$ is incremental thermal strain vector and can be given as:

$$\Delta \varepsilon_{thermal} = \Delta {\theta_e}^k \alpha \quad \{9\}$$

where $\Delta {\theta_e}^k$ is the incremental change in element temperature for k^{th} time step and α is the vector for the roll material's coefficients of thermal expansion assuming orthotropic material:

$$\Delta {\theta_e}^k = {\theta_e}^k - {\theta_e}^{k-1} \quad \{10\}$$

$$\alpha = [\alpha_r \quad \alpha_z \quad 0 \quad \alpha_\theta]^t \quad \{11\}$$

If we have a temperature time series, defining the thermal process with starting with the initial element temperature ${\theta_e}^0$, then {8}, {9} and {10} will be written for $k=1,2,...,n_T$. Here $n_T + 1$ is the number of elements in the time temperature series including ${\theta_e}^0$. M^{k-1} is the element material stiffness matrix for step *k-1* with the nonlinear part (radial modulus) is calculated with ${\sigma_e}^{k-1}$ which is the current total stress as $\Delta \sigma^k$ is yet to be known. Now it is understood that:

$$\sigma_e^k = {\sigma_e}^{k-1} + \Delta {\sigma_e}^k \quad \{12\}$$

And ${\sigma_e}^0$ is the element initial stress vector at the beginning of the thermal analysis i.e winding stresses at the end of the winding. This step-wise approach can be easily

installed into a finite element frame as before. Applying integral form of virtual work on an element:

$$\int_{V_e} \left(\Delta\sigma_e^{\,k}\right)^T \delta\Delta\varepsilon^k dV = 0 \qquad \{13\}$$

Now usual finite element equations can be easily derived by employing the same isoparametric formulation given in axisymmetric winding model:

$$K_e^{k-1}\Delta u^k{}_e = F_{\theta e}^k \qquad \{14\}$$

$$K_e^{k-1} = \int_{-1}^{1}\int_{-1}^{1} B^T \left(M^{k-1}\right)_e B \det[J] r d\eta d\xi \qquad \{15\}$$

$$F_{e\theta}{}^k = \Delta\theta_e^k \int_{-1}^{1}\int_{-1}^{1} B^T \alpha \det[J] r d\eta d\xi \qquad \{16\}$$

Elemental equation {12} is used to obtain system of equations for whole roll body including the core. Solution to this system gives the incremental displacements for step *k*. Incremental stresses are then calculated per equation {12}. The complete solution algorithm is given in Table 1.

process #	definition
1	input geometrical, material data and initial stresses σ^0 corresponding to initial temp. θ^0 , temp-time series (θ^0, θ^1,.., θ^{nT}) for all nodes and elements
2	Do for $k=1$ to n_T
2.1	form finite element equations using equations {15} and {16} for all elements (including core)
2.2	assemble and solve system of equations and obtain incremental displacements Δu^k , calculate incremental strains $\Delta\varepsilon^k$ and calculate incremental stresses $\Delta\sigma^k = M^{k-1}(\Delta\varepsilon^k - \Delta\varepsilon_{thermal})$ for all elements
2.3	update stresses $\sigma^k = \sigma^{k-1} + \Delta\sigma^k$
2.4	update radial modulus $E_r{}^k = K_2(-\sigma_r{}^k + K_1)$
3	print results (stresses and strains for *each step*)

Table 1 – Algorithm for Thermo-elastic Solution

TRANSIENT HEAT TRANSFER ANALYSIS OF A WOUND ROLL

Most of the time roll production is completed under isothermal conditions. After production stage, transportation and storage temperatures might be quite different and roll immediately begins to move to thermal equilibrium via various types of heat diffusion processes. In this work we will assume that roll is produced with an initial body temperature of T^0 and then put in an ambient homogeneous temperature medium with temperature T^∞. As roll body temperature inhomogeneously moves from T^0 to T^∞ fundamental effect of heat transfer is assumed to be of convection type. Per consistency with the winding stress model, roll is assumed to be a hollow cylinder with a core. Perfect

conduction is assumed between core and the layers above. Now the basic problem is to calculate the temperature time series of an axisymmetric body under convection conditions. In the absence of internal heat generation, axisymmetric form of heat transfer equation for an orthotropic material is given as:

$$\rho c \frac{\partial T}{\partial t} = \frac{1}{r}\frac{\partial}{\partial r}\left(k_r r \frac{\partial T}{\partial r}\right) + \frac{\partial}{\partial z}\left(k_z \frac{\partial T}{\partial z}\right) \quad \{17\}$$

where ρ and c are mass density and specific heat capacity respectively. k_r and k_z are thermal conductivities along radial and axial directions respectively. In this study they are assumed to be functions of position i.e. can vary spatially. Since we assume convection type boundary conditions for all surfaces of the cylinder, boundary condition can be stated as:

$$q_c = h_c(T^{\infty} - T^S) \quad \{18\}$$

where q_c is the convection based heat flux along normal direction to the boundary (positive if entering the body), h_c is the heat transfer coefficient and T^S is the boundary temperature of the immersed body that is wound roll's surface temperature. We assume a homogeneous body temperature at the beginning because of the isothermal production environment so T^S at the beginning is simply the initial homogeneous roll body temperature T^0. Although heat transfer coefficient h can be a function of temperature and geometry at times for extreme thermal gradients, for cooling and heating around room temperature it is taken constant in this study. As we begin with the winding stress analysis we can extend the already constructed finite element frame for the solution of heat transfer equation. This will be convenient as the element based geometrical and material data is already coming from winding stress model. With this idea Figure 4 shows the winding model and heat transfer model side by side. All the element information from winding model can be used to construct the heat transfer model. Here in order to facilitate calculations an increase computational efficiency an additional simplification can be made: As seen from Figure 4 instead of using the general quadrilateral elements of winding model heat transfer model can be constructed from rectangular elements positioned at the same location. Since variations in thickness is unessential for heat transfer analysis (whereas in stress analysis wide-wise thickness distribution is crucial) we can represent a stress element (with variable side thickness refer to Figure 2) with a heat transfer element which has the same width but constant thickness. This constant thickness can be taken as the average thickness of the corresponding layer of finite elements in stress model.

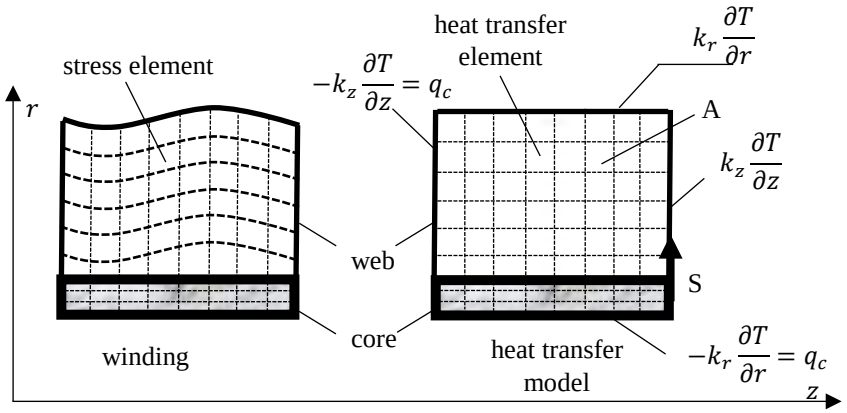

Figure 4 – Winding Model Based Heat Transfer Model

Figure 4 also shows the convection based heat flux boundary conditions for the entire wound roll where q_c is given by {18}. Transient heat transfer analysis using finite elements is well established in the literature and here we will only cover essentials for the sake of completeness. The same isoparametric finite element formulation can be utilized for heat transfer problem by using the 4-node rectangular elements and the associated shape functions. Formulation will begin by deriving the virtual heat equilibrium. Using the virtual temperature field which satisfies prescribed temperature boundary conditions we can write down the weighted residual form of {17}:

$$\int_V \left(\rho c \frac{\partial T}{\partial t} - \frac{1}{r}\frac{\partial}{\partial r}\left(k_r r \frac{\partial T}{\partial r} \right) - \frac{\partial}{\partial z}\left(k_z \frac{\partial T}{\partial z} \right) \right) (\delta T)\, dV = 0 \qquad \{19\}$$

Integrating {19} on derivatives of T by parts, applying Divergence theorem on the resulting volume integrals and using $dV = 2\pi r dA$ we arrive at the following summation over elements:

$$\sum_e \left(\int_{A_e} \left((\rho c)_e \frac{\partial T}{\partial t}\delta T + \left(k_{re} \frac{\partial T}{\partial r}\frac{\partial \delta T}{\partial r} + k_{ze} \frac{\partial T}{\partial z}\frac{\partial \delta T}{\partial z} \right) \right) 2\pi r dA - \int_{S_s} (\delta T) q_c 2\pi r dS \right) = 0 \qquad \{20\}$$

The main assumption is the separation of the time and spatial portions of the temperature field. This separation allows us to introduce finite element approximation of the temperature field in a natural manner by assuming the nodal values as time dependent only. Then the shape functions which are defined over element with local coordinates ($\bar{r}, \bar{z}$ located at the center of an element) are used to construct the actual and virtual field approximation over an element:

$$T_e(t, \bar{r}, \bar{z}) = \sum_{i=1}^{4} \theta_{ie}(t) \phi_i(\bar{r}, \bar{z}) \qquad \{21\}$$

$$\delta T(t, \bar{r}, \bar{z}) = \sum_{i=1}^{4} \delta\theta_i(t) \phi_i(\bar{r}, \bar{z}) \qquad \{22\}$$

Here θ_{ie} and ϕ_i are i[th] nodal temperature at time t and corresponding shape function respectively. Substituting {21} and {22} into {20}, using convection boundary condition {18} and invoking the conservation of thermal energy by the arbitrariness of virtual temperatures we arrive:

$$C_e\dot{\theta}_e + \hat{K}\theta_e = f_e \qquad \{23\}$$

where

$$C_{eij} = (\rho c)_e \int_{A_e} \phi_i \phi_j r d\bar{r} d\bar{z}$$

$$\hat{K}_{eij} = k_{re} \int_{A_e} \frac{\partial \phi_i}{\partial \bar{r}} \frac{\partial \phi_j}{\partial \bar{r}} r d\bar{r} d\bar{z} + k_{ze} \int_{A_e} \frac{\partial \phi_i}{\partial \bar{z}} \frac{\partial \phi_j}{\partial \bar{z}} r d\bar{r} d\bar{z} + h_c \int_{S_e} \phi_i \phi_j r ds$$

$$f_{ei} = T^{\infty} h_c \int_{S_e} \phi_i r ds$$

C_e is element capacitance matrix, $\hat{K}_e$ is augmented element conductance matrix, as observed, last term including the boundary integral will apply only for the elements which have boundaries overlapping with S. Again the element thermal load term f_e will be only calculated for these boundary elements' overlapping boundaries with S. It is also worth mentioning that by setting h_c to a very large number (e.g. 10^{20}) prescribed temperature type boundary conditions can also be modeled. This will correspond to a multipoint constraint type formulation which is forcing the nodes on the boundary S to be equal to ambient temperature T^{∞}. The integrals appearing in {23} can be analytically calculated since we have constructed the model over the rectangular elements (ref. Figure 4). Now the usual finite element assembly procedure can be applied over elements and the system of equations can be obtained as an ordinary differential equations of time:

$$C\dot{\theta} + \hat{K}\theta = f \qquad \{24\}$$

Equation {24} can be integrated over time with various methods. Here we selected Crank-Nicolson type approximation which is unconditionally stable. Starting from time $t^0=0$, taking the final time as t^f and defining the time increment with $\Delta t=(t^f-t^0)/n_t$ a discrete time series can be defined. Then Crank-Nicolson approximation can be given as:

$$(C + \Delta t\hat{K}/2)\theta^k = (C - \Delta t\hat{K}/2)\theta^{k-1} + f \qquad \{25\}$$

where k is time step counter from 1 to total number of time steps n_t ($k=1,2,..,n_t$) and θ^k is the nodal temperature vector at time step k ($t^k=t^0+k\Delta t$). Initial temperature vector is simply taken as the initial roll body temperature i.e. $\theta^0 = T^0$. Notice that C, $\hat{K}$ and f are time independent. A code is developed for the finite element heat-transfer problem based on the formulation above. Representative results are used to demonstrate the validity in which we compare code results with finite element package ABAQUS. A cylindrical body (PET wound roll) with a steel core is assumed to be homogeneously have an initial temperature of 21.1 ˚C (70 ˚F) put into an environment with an ambient temperature of

37.8 ˚C (100 ˚F). Related data is for PET and steel core is given in Table 2. As seen from Figure 5 calculated results are very close to the ABAQUS results.

Geometry		Bulk		Thermal	
in. r_{core} (cm)	5	$\rho_{core}(gr/cm^3)$	7.85	$k_{core}(W/m.K)$	30
in. r_{roll} (cm)	10	$c_{core}(J/gr\ K)$	0.5	$k_{rweb}(W/m.K)$	0.2
out. r_{roll} (cm)	40	$\rho_{web}(gr/cm^3)$	1.34	$k_{zweb}(W.m.K)$	0.2
width (cm)	60	$c_{web}\ (J/gr\ K)$	1	$h_c\ (W/m^2.K)$	5

Table 2 – Material Data for Heat Transfer Simulation

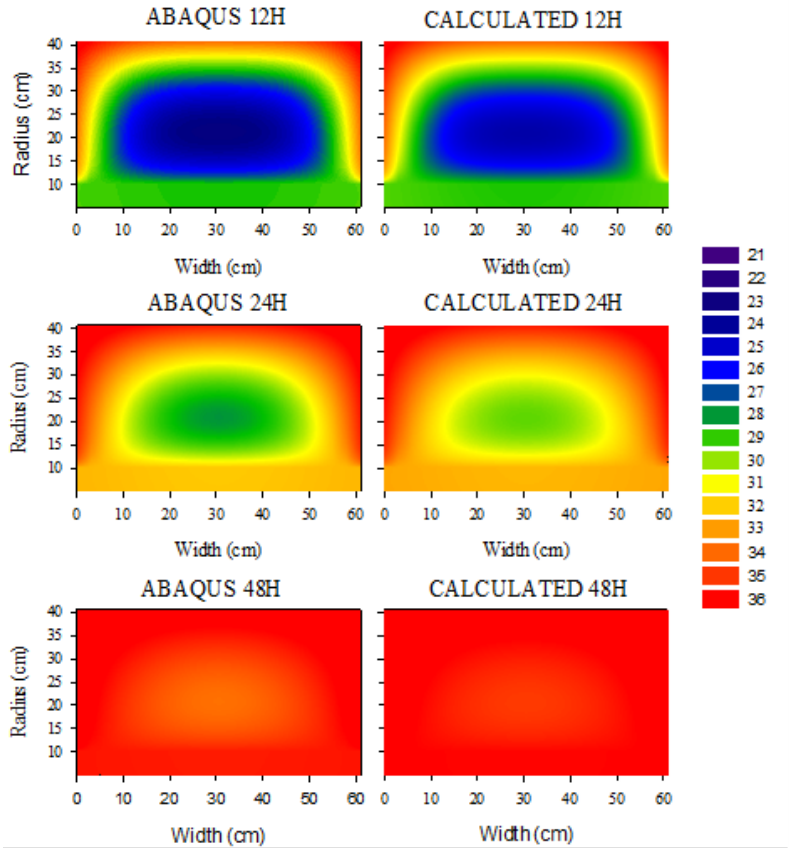

Figure 5 – ABAQUS and Heat Transfer Model Temperatures (˚C) Comparison

INTEGRATED TRANSIENT THERMO-ELASTIC ANALYSIS

In this section we will merge the winding model and the heat transfer model via thermo-elastic model. Since the system is uncoupled, that is none of the heat transfer parameters are stress state dependent we will basically apply the models consecutively. First for a given winding parameter set (material properties, winding tension etc.) the roll will be wound, that is stress state will be determined. Concurrently the transient

calculations will be completed independently. A time series consisting of the nodal temperature vectors corresponding to discrete time steps will be produced. Element temperatures will be then obtained by averaging the nodal temperature vector over elements. Now the thermo-elastic model can be used by calculating the incremental thermal strains from the element temperature difference between two consecutive time steps and the corresponding thermal stresses can be obtained by the thermo-elastic model. The general algorithm is given in Table 3.

process #	definition
1	input geometrical and material (mechnical and thermal) data
2	use winding model to obtain initial stresses $\sigma_{rz}^{\ 0}$ $\sigma_r^{\ 0}$, $\sigma_\theta^{\ 0}$, $\sigma_z^{\ 0}$
3	for a given ambient temperature T^∞, homogeneous body temperature T^0 and duration t_f, time increment $\Delta t=t_f/n_t$ calculate nodal temperature vectors θ^k with $\theta^0=T^0$, for $k=1,2,..,n_t$ using transient heat model
4	Select n_T nodal temperature vector and calculate element temperatures $\theta_e^{\ k}$ from selected nodal temperature vectors by averaging over element
5	feed initial stresses σ^0 and element temperatures $\theta_e^{\ k}$ for $k=0,1,2,..,n_T$ into the thermo-elastic algorithm given in Table 1.

Table 3 – Integrated Algorithm for Transient Thermo-elastic Stress Analysis

As noticed number of time steps n_t and the number of temperature increments n_T can be different. In fact one can select $n_T=n_t$ and use all of the transient temperature vectors for rapid temperature changes or can select some of them (e.g. selecting $n_T=n_t/10$ thus taking temperature vectors for thermo-elastic calculations at every $10\Delta t$ interval).

RESULTS AND CONCLUSIONS

First results will be related with the validation of the thermo-elastic stress analysis. Only wound roll thermo-elastic experiments in the literature are due Qualls & Good [2]. They have developed methods for measuring the thermal expansion coefficients and used parameters in their 1D model for predicting in-roll pressures of a roll wound by LDPE. They wound the roll in isothermal conditions (room temperature) with pull-tabs inserted at certain radial locations. After winding first they measured radial pressures at room temperature and then placed the roll into a controlled environment with a different temperature and allowed it to reach thermal equilibrium for 24 hours. The results taken after this period are used to validate the thermo-elastic model. They used three different ambient temperatures (T^∞=26.5, 32.1, 37.6 ˚C). Web tension during winding was T_w=690 KPa. Material data is given in Table 4.

Geometry & Mechanical		Bulk & Thermal	
in. r_{core} (cm)	4	$\rho_{core}(gr/cm^3)$	7.85
in. r_{roll} (cm)	4.45	$c_{core}(J/gr\ K)$	0.5
out. r_{roll} (cm)	13.45	$\rho_{web}(gr/cm^3)$	0.92
width (cm)	15.2	$c_{web}\ (J/gr\ K)$	2
K_1 (MPa)	0	$k_{core}(W/m.K)$	30
K_2	167	k_{zweb},$k_{rweb}(W/m.K)$	0.33
E_θ, E_z (MPa)	172.4	$h_c\ (W/m^2.K)$	5
v_{rz} $v_{\theta r}$, $v_{\theta z}$	0.3	$\alpha_r(1/C)$	$1.01x10^{-4}$
E_c (GPa)	200	α_θ, $\alpha_z(1/C)$	$3.35x10^{-4}$
v_c	0.3	$\alpha_{core}(1/C)$	$1.08x10^{-5}$

Table 4 – LDPE Material Data for Comparison with Qualls & Good [2]

Isotropic representative values for coefficient of thermal conductivity is used for the calculations. Selected heat transfer coefficient is h_c typical for convection process of horizontal cylinder in air. In the numerical solution t_f=1440 min (24 h.), Δt=1 min. is used. Every transient step is used for stress calculation i.e. $n_T=n_t$.

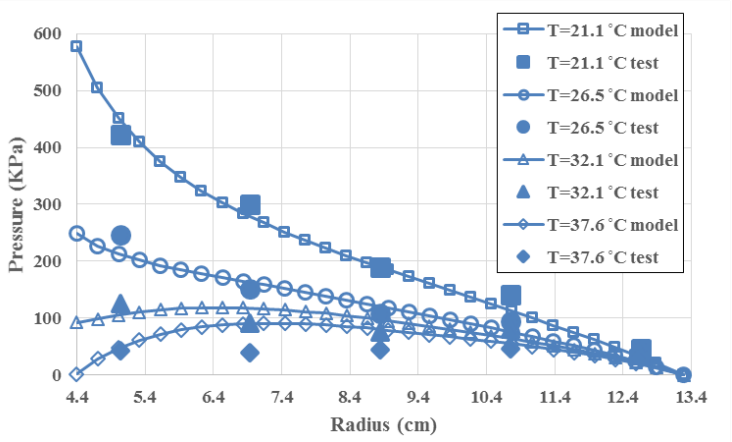

Figure 6 – Heat Transfer Model Predictions

Figure 6 shows the thermo-elastic model results with the experimental results. Predictions of the model matches reasonably well with the experimental results and this is an indication of the successful integration of the transient model with the thermo-elastic winding model. Figure 7 shows the temperature distributions of the wound roll used in the verification for T^∞=37.6 ˚C ambient temperature. As seen from Figure 7 even a duration of 12 hours is almost enough for thermal equilibrium for this relatively small roll with assumed thermal properties.

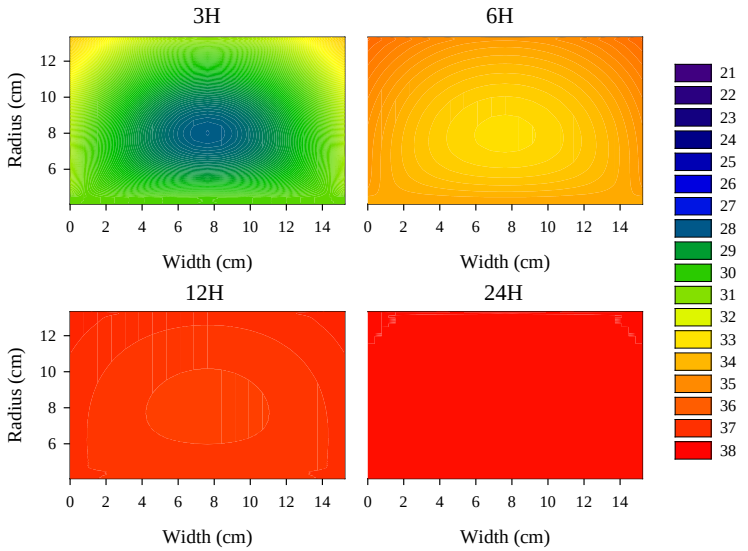

Figure 7 – Heat Transfer Model Temperature Distribution (˚C)

In literature there is not any known thermo-elastic winding experiment concerning the axisymmetric stress distribution. In order to demonstrate numerical results from this study we considered a fictitious roll wound from 300 gage PET with machine direction persistent thickness variation. We used the same thermal properties given in Table 2 for this PET as well. All related data is given in Table 5. Thermal expansion coefficients are assumed to be similar to LDPE.

Geometry & Mechanical		Bulk & Thermal	
in. r_{core} (cm)	9.5	$\rho_{core}(gr/cm^3)$	7.85
in. r_{roll} (cm)	10	$c_{core}(J/gr\ K)$	0.
out. R_{roll} (cm)	20	$\rho_{web}(gr/cm^3)$	1.34
width (cm)	60	$c_{web}\ (J/gr\ K)$	1
K_1 (Mpa)	0	$k_{core}(W/m.K)$	30
K_2	246.5	k_{zweb},$k_{rweb}(W/m.K)$	0.2
E_θ, E_z (Mpa)	5000	$h_c\ (W/m^2.K)$	5
v_{rz} $v_{\theta r}$, $v_{\theta z}$	0.3	$\alpha_r(1/C)$	$1.01x10^{-4}$
E_c (Gpa)	200	α_θ, $\alpha_z(1/C)$	$3.35x10^{-4}$
v_c	0.3	$\alpha_{core}(1/C)$	$1.08x10^{-5}$

Table-5 – PET Material Data for Axisymmetric Stress Results

Fictitious roll is assumed to be wound with a web-line tension of T_w=2.3 MPa in room temperature (T^0=21.1 ˚C) and then placed into an environment with constant ambient temperature of T^∞=10 ˚C. Assumed MD persistent thickness profile and core pressures corresponding to initial and later transient times are given in Figure 8.

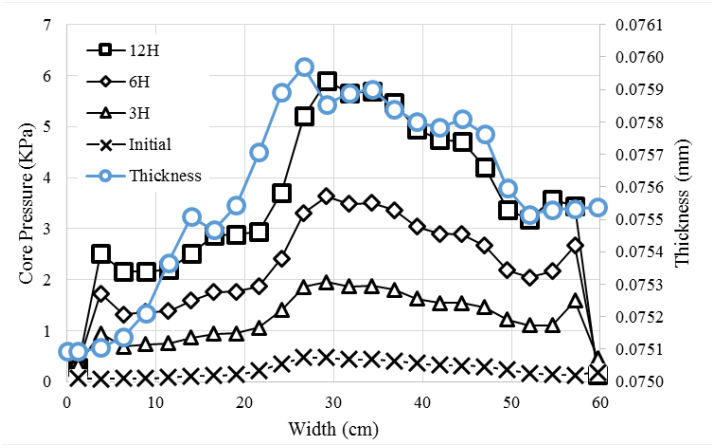

Figure 8 – Core Pressure Comparison for Pet Roll (Table 5)

From Figure 8, as expected, core pressure is increasing with decreasing temperatures. The non-uniformity of the pressure profile is directly related with the non-uniform thickness profile. Figure 9 shows results for radial pressures for axisymmetric case. It is seen that significant levels of pressure build up occurs during cooling around steel core. This was expected since radial coefficient of thermal expansion used for PET is one order greater in magnitude than the steel core's coefficient of thermal expansion.

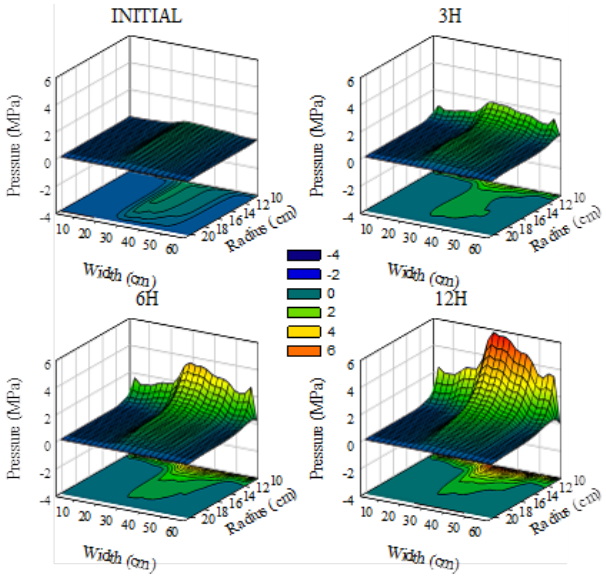

Figure 9 – Radial Pressure Field Results for Initial, 3, 6, and 12 H. Transient Durations

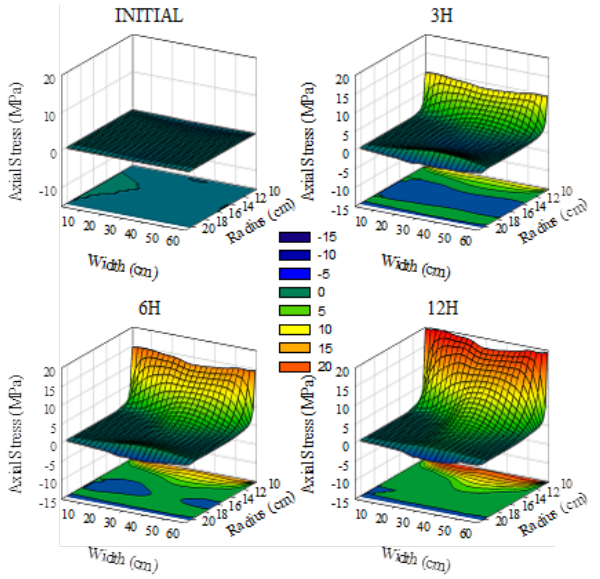

Figure 10 – Axial Stress Field Results for Initial, 3, 6, and 12 H. Transient Durations

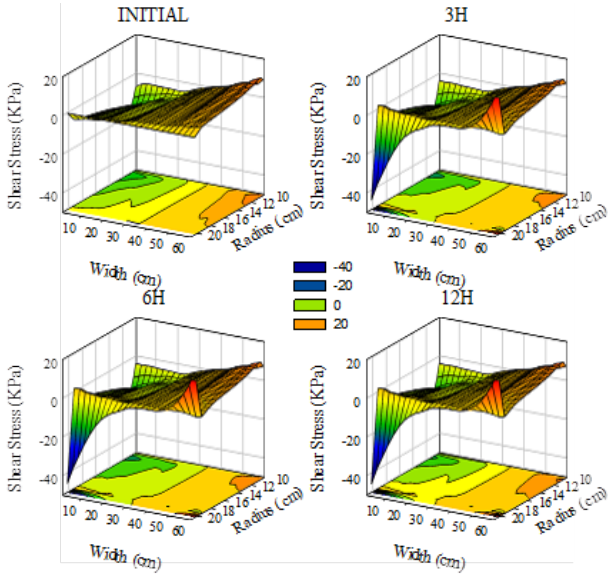

Figure 11 – Shear Stress Field Results for Initial, 3, 6, and 12 H. Transient Durations

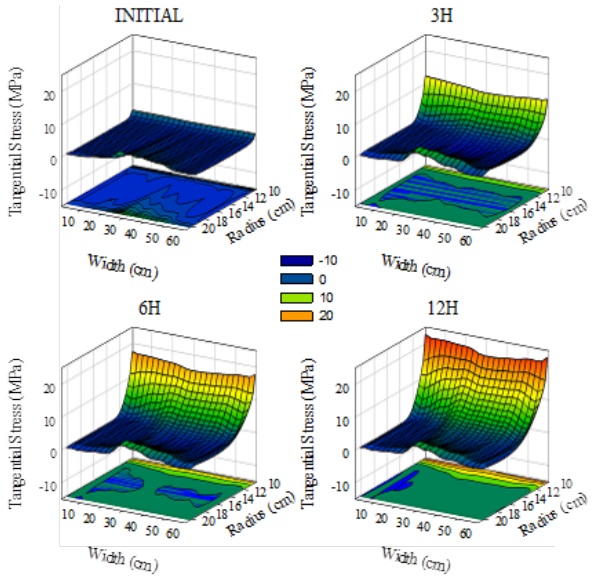

Figure 12 – Tangential Stress Field Results for Initial, 3, 6, and 12 H. Transient Durations

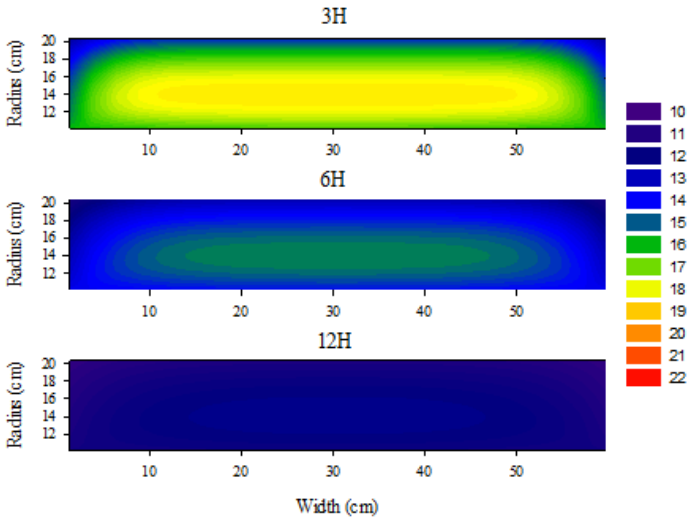

Figure 13 – Transient Temperature Results (˚C) for 3, 6, and 12 H. Transient Durations

Figure 10 shows results for axial stresses. Again because of thermal expansion of coefficient mismatch between PET and steel causes significant axial stresses. Shrinkage of web layers around core vicinity are one order of magnitude greater than the steel core's shrinkage. Figure 11 shows results for shear stresses they seem to be less effected by the temperature change. Indeed primary effect of temperature is change in volumetric strain hence shear strains are changed almost entirely because of mechanical equilibrium. Figure 12 shows the tangential stresses and like axial stresses significant values are

attained around core vicinity. This is again the primary results of coefficient of thermal expansion mismatch as the web layers shrinkage along radial direction is constrained by the less contracting core. Therefore tangential strains and stresses build up. Finally Fig 13. Shows the transient temperature distribution corresponding to 3, 6, 12 H. transient durations. It is observed that 12 H. duration can be assumed as the required time to reach thermal equilibrium for the roll under consideration. In the calculations we used isotropic uniform thermal expansion of coefficient for web. In fact this well be a state dependent property especially for radial direction as the pressure changes the asperity contact conditions hence effects conductivity. The proposed model is uncoupled (that is conductivity is not changing with temperatures) but results concerning the spatial non-uniform distribution of thermal conductivity can be obtained. As an initial approximation of pressure dependence we can assume that the thermal conductivity in radial direction is dependent upon initial pressure distribution. No known study exist in the literature about the exact nature of this relation. Here in order to show non-uniform thermal conductivity feature it is assumed that spatial thermal conductivity distribution in radial direction has an exponential relation with the radial pressure:

$$k_r(P_{ini.}) = k_{rbulk}(P_{ini.} / P_{ini.max})^{\lambda} \qquad \{26\}$$

Here k_{rbulk} will be taken as the indicated material thermal conductivity of the web material itself. Thus $k_r(P_{ini.})$ function defines the spatial distribution of thermal conductivity for wound roll structure depending on the initial local pressure $P_{ini.}$ which directly coming from winding process. $P_{ini.max}$ is selected as the maximum value of pressure at the end of the winding process somewhere on the core. Finally λ is a constant which controls the intensity of the effect of pressure distribution over thermal conductivity and $0 \leq \lambda \leq 1$. Now it is obvious that k_r attains its max value as the bulk thermal conductivity k_{rbulk} where initial maximum pressure occurs i.e. where $P_{ini.} = P_{ini.max}$. Notice that $\lambda = 0$ corresponds to the constant thermal conductivity case.

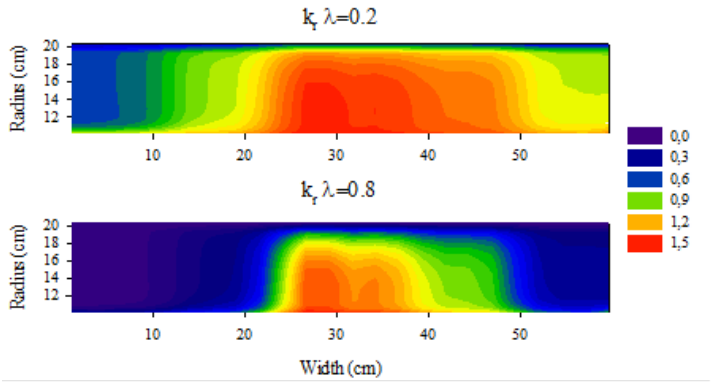

Figure 14 – k_r Distribution w/ Expression {26}

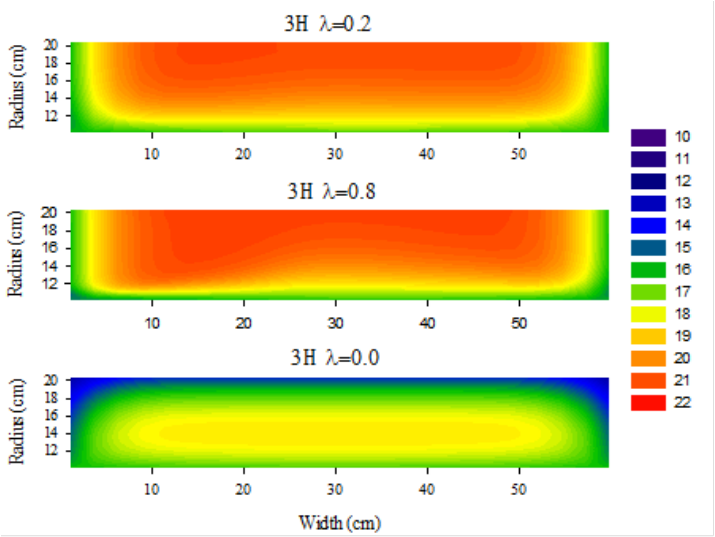

Figure 15 – Transient Temperature Results (˚C) for 3H Duration and λ=0.2, 0.8, 0.0

Figure 14 shows k_r distributions for $k_{rbulk}=1.5$ and $\lambda=0.2, 0.8$. Figure 15 shows corresponding transient temperature results for given values of λ. Clearly indicating the effects of pressure dependent inhomogeneous orthotropic k_r. Low values of k_r causing the slower cooling of the low pressure areas of the inner roll. Figs. 16, 17 and 18 show corresponding radial pressure, axial and tangential stress distributions respectively. It is observed from graphs pressure dependent orthotropic k_r plays a crucial role on the in-roll stresses. Pressure distribution seems to be tending smoother for inner roll regions as the inner temperatures are less affected because of low k_r values occurring for this region. Again for axial and tangential stresses difference between outer surface temperature and inner regions causes remarkable effects. Outer layers tend to shrink more in radial and axial directions and this is causing stress build up at outer sections of the roll. Expression {26} is just introduced to show the orthotropic feature of the formulation. The most important conclusion is understanding the need of a fully coupled thermo-elastic transient model (a truly multi-physics model) which includes a physically sound relation between thermal conductivity and pressure. This requires experimental work for the determination of this relation. We can consider a stack of web which is embedded with thermocouples and applied a known pressure. If the stack's sides are insulated, a heat source from bottom face of the stack would be used to introduce transient temperature field which can be monitored with thermocouples. An inverse heat transfer problem can be applied for this system in order to infer the k_r dependence on pressure. The layer-wise structure of the wound roll clearly indicates the need of this type of orthotropic nonlinear transient response which is coupled with the winding model. The model predictions for relatively narrow webs (as in used verification [2]) agree reasonably well because cooling and heating of these kind of small rolls, in general, approach to ideal case of homogeneous temperature distributions. Nevertheless a fully coupled transient model would be more appropriate to distinguish the "small" or "large" roll with respect to thermo-elastic effects as a "large" roll with high k_r would tend to behave closer to the ideal homogeneous case than a "small" roll with low k_r and vice versa.

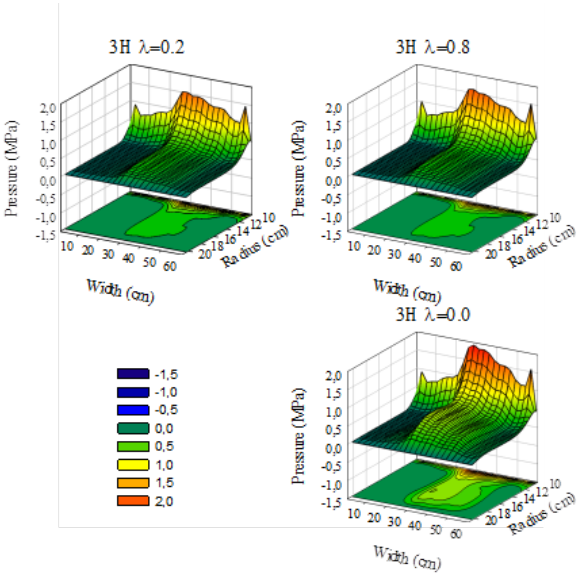

Figure 16 – Pressure Results (˚C) for 3H Duration and λ=0.2, 0.8, 0.0

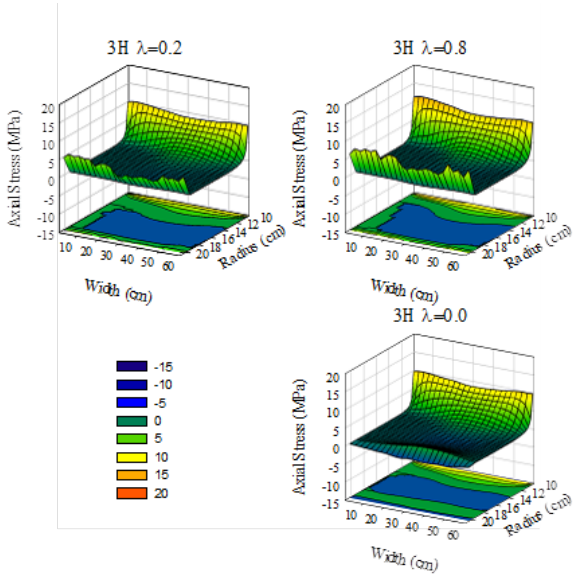

Figure 17 – Axial Stress Results (˚C) for 3H Duration and λ=0.2, 0.8, 0.0

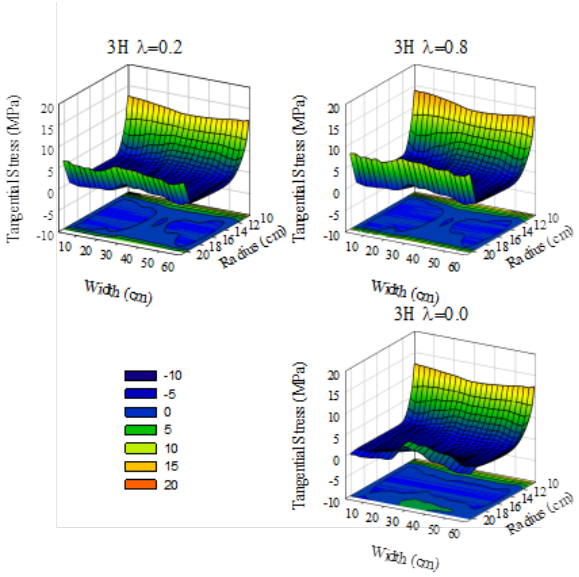

Figure 18 – Tangential Stress Results (˚C) for 3H Duration and λ=0.2, 0.8, 0.0

REFERENCES

1. Qualls, W. R., and Good, J. K., "Thermal Analysis of a Round Roll," Journal of Applied Mechanics-Transactions of ASME , Vol. 64, No. 4, Dec. 1997, pp. 871-876.
2. Mollamahmutoglu, C., and Good, J. K., "Modeling the Influence of Web Thickness and Length Imperfections Resulting from Manufacturing Processes on Wound Roll Stresses," Journal of Manufacturing Science and Technology, Vol. 8, Jan. 2015, pp. 22-33.
3. Cole, K. A., and Hakiel, Z., "A Nonlinear Wound Roll Model Accounting for Widthwise Web Thickness Nonuniformities," Proceedings of the Web Handling Symposium, ASME Applied Mechanics Division, Vol. 149, 1992, pp.13-24.
4. Lee, Y. M., Wickert, J. A., "Stress Field in Finite Width Axisymmetric Wound Rolls," ASME Journal of Applied Mechanics, Vol. 69, No. 2, March 2002, pp. 130-138.
5. Arola, K., and von Hertzen, R., "Two Dimensional Axisymmetric Winding Model for Finite Deformation," Computational Mechanics, Vol. 40, Issue 6, Nov. 2007, pp. 933–947.
6. Mollamahmutoglu, C., Good, J.K., "Analysis of Large Deformation Wound Roll Models," ASME Journal of Applied Mechanics, Vol. 80, No. 4, May 2013, pp. 041016-1–041016-11.